Iridium Oxide-Based Potassium Sensitive Microprobe With Anti-Fouling Properties

Krzysztof Wildner, Khalid Baig Mirza, *Member, IEEE*, Brian de La Franier, Simon Cork, Christofer Toumazou, *Fellow, IEEE*, Michael Thompson, *Member, IEEE*, and Konstantin Nikolic, *Member, IEEE*

***Abstract*—Here, we present a new type of potassium sensor which possesses a combination of potassium sensing and anti-biofouling properties. Two major advancements were required to be developed with respect to the current technology; Firstly, design of surface linkers for this type of coating that would allow deposition of the potassium-selective coating on Iridium (Ir) wire or micro-spike surface for *chronic* monitoring for the first time. As this has never been done before, even for flat Ir surfaces, the material's small dimensions and surface area render this challenging. Secondly, the task of transformation of the coated wire into a sensor. Here we develop and bench-test the electrode sensitivity to potassium and determine its specificity to potassium versus sodium interference. For this purpose we also present a novel characterisation platform which enables dynamic characterization of the sensor including step and sinusoidal response to analyte changes. The developed sensor shows good sensitivity (<1 mM concentrations of K^+ ions) and selectivity (up to approximately 10 times more sensitive to K^+ than Na^+ concentration changes, depending on concentrations and ionic environment). In addition, the sensor displays very good mechanical properties for the small diameter involved (sub 150 μm), which in combination with anti-biofouling properties, renders it an excellent potential tool for the chemical monitoring of neural and other physiological activities using implantable devices.**

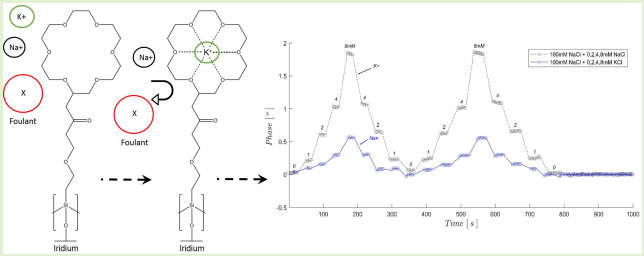

***Index Terms*— Potassium sensing, anti-fouling, surface linker, iridium oxide, impedance spectroscopy, neurochemical measurements.**

I. Introduction

ABNORMAL values of potassium (K^+) concentration in tissue have been associated with several conditions such as epilepsy, neuromuscular ataxia, cardiac arrhythmia, and Alzheimer's disease [1]. This observation, in addition to fundamental studies in neuroscience, has resulted in attempts to monitor the *in vivo* concentration of the cation. Such measurements involving standard glass microelectrodes dates to the 1970s [2], [3]. More recent times have seen the introduction of probes based on optical science such as the micro-optrode or fluorescence spectroscopy [4], [5]. The aim of the present work is to investigate the possibility of creating a potassium sensor based on an Iridium substrate. This is prompted by the successful testing and demonstration of the closed-loop capabilities for pH sensing achieved using IrOx microelectrodes [6], [7]. Such an approach should offer additional benefits such as greater temporal and spatial resolution of neural activity, including the peripheral nervous system. In addition, it also offers the possibility to chronically record cation concentration as an implantable sensor. Until recently, this was unachievable due to the lack of sufficiently hard K^+ sensitive substrates within such a small form factor. Several techniques, such as ionophore entrapment within polyphenol coatings on Pt microelectrodes, with Ni hexacyanoferrate layers using carbon screen printed electrodes (PEDOT doped with ATP) have been attempted but failed to function [8].

As mentioned above, the standard technique for detecting potassium ions is to use a glass capillary electrode (a pipette)

Manuscript received March 24, 2020; revised June 11, 2020; accepted June 12, 2020. Date of publication June 17, 2020; date of current version October 2, 2020. This work was supported in part by the U.K. Engineering and Physical Sciences Research Council (EPSRC) Grant EP/N002474 and in part by the ERC Synergy Grant 319818. The associate editor coordinating the review of this article and approving it for publication was Dr. Gymama Slaughter. *(Corresponding author: Khalid Baig Mirza.)*

Krzysztof Wildner was with the Department of Electrical and Electronic Engineering, Imperial College London, London SW7 2AZ, U.K. He is now with the Institute of Metrology and Biomedical Engineering, Warsaw University of Technology, 02-525 Warsaw, Poland.

Khalid Baig Mirza and Christofer Toumazou are with the Department of Electrical and Electronic Engineering, Imperial College London, London SW7 2AZ, U.K. (e-mail: k.mirza@imperial.ac.uk).

Brian de La Franier and Michael Thompson are with the Department of Chemistry, University of Toronto, Toronto, ON M5S 3H6, Canada (e-mail: m.thompson@utoronto.ca).

Simon Cork was with the Department of Metabolism, Digestion and Reproduction, Hammersmith Hospital, Imperial College London, London W12 0NN, U.K. He is now with the GKT School of Medical Education, King's College London, London SE1 1UL, U.K.

Konstantin Nikolic was with the Department of Electrical and Electronic Engineering, Imperial College London, London SW7 2AZ, U.K. He is now with the School of Computing and Engineering, University of West London, London W5 5RF, U.K. (e-mail: konstantin.nikolic@uwl.ac.uk).

Digital Object Identifier 10.1109/JSEN.2020.3003040

with a gradient cation-sensitive ionophore and a carbon fiber conductive wire [9]. However, these sensors are fragile and bulky, not biocompatible, and cause inflammation when used as potential implants or in *in vivo* preparations. Another option is to make a 'solid-state' electrode, but the issue in this case is that the ionophore layer which is specific to potassium ions becomes saturated for very low potassium concentrations and needs a 'protective' layer above it. Furthermore, current technologies can only produce a minimum thickness of about 200μm, which is far too thick for many applications involving the peripheral and central nervous system. Given these issues, the employment of Ir-based electrodes offers attractive potential for the detection of K^+. The overall aim is to develop electrodes that are thin (sub-150 μm diameter) such as a micro-spike, which can be scaled up to a length of about 1cm. The devices must be mechanically stable enough to penetrate the epineurium and perineurium of the nerves or brain membranes, with tight coupling to nerve axons, or be placed in the extracellular space in the brain. Iridium is a biocompatible material which has very good mechanical and electrical properties. These properties are crucial for measuring potassium concentration inside tissue. Iridium micro-wires have been used previously to interface with peripheral nervous system by fabricating and demonstrating a pH sensor which reliably detects *in vivo* neural activity, with much better signal to noise ratio (SNR) and much less interferences than electrical recordings [6], [7].

A strategy for the development of a potassium-specific Iridium electrode is offered by a recently developed biosensor employed for *in vivo* measurement in a mouse cranium for measurement of K+ concentration [10]. In this work, a monolayer on a planar gold microelectrode surface for K^+ sensitivity was fabricated with capabilities for tandem anti-fouling [11], [12] and selective potassium binding via a crown ether [13]. An analogous anti-fouling layer, based on trichlorosilane linking chemistry, has also been developed which is capable of being attached to medical-grade stainless steel [14]. Based on this approach, a further anti-fouling molecule, 3-(3-(trichlorosilyl)propoxy)propanoyl chloride (MEG-Cl), which incorporates an acid chloride end group for linking to other compounds, has also been developed [15]. This chemistry allows the possibility to attach a MEG-Cl monolayer to Iridium, which can then be extended with 18-crown-6 ether to introduce K^+-sensitivity to the substrate (Fig. 1).

Successful development of this micro-sensor enables the fabrication of a fully functional *bimodal* platform that will utilize both chemical and electrical recordings of neural activity. Such sensory capability can be combined with a signal processing and decision algorithm, and stimulation module. These technologies together with the attractive possibility to form a novel closed-loop stimulation system will allow the opportunity to answer two main questions for closed-loop stimulation, that is, *when* to stimulate as well as the type of stimulation *dosage* invoked [16]–[18]. The sensor can be readily extended into sensor arrays [19], [20].

II. Experimental

A. Materials

3-(3-(Trichlorosilyl)propoxy)propanoyl chloride (MEG-Cl) was synthesized according to previously published methods [10]. All chemicals were purchased from Sigma–Aldrich (St. Louis, MO, USA). Epoxy Araldite (ARA400012) was purchased from Farnell (UK). This epoxy is non-biocompatible. A biocompatible epoxy such as EPO-TEK MED-310-2 could also be used in future.

B. Cleaning and Surface Modification of Iridium Wire

Iridium plates (1cm x 1cm, for XPS analysis) or a section of iridium wire (125 μM diameter) were sonicated successively in pentane, acetone, and 95% ethanol for 15 minutes each. The iridium was then rinsed copiously with 95% ethanol followed by deionized water. The iridium was then submerged in piranha solution (3:1 sulphuric acid:30% hydrogen peroxide) for 30 minutes at 90°C. It was then rinsed copiously with deionized water followed by methanol, and then placed in an oven at 180°C for 2 hours to dry the surfaces. The iridium was then plasma cleaned under atmosphere for 5 minutes. Finally, it was stored overnight in a humidity chamber at 80% humidity to saturate the surface with water.

The iridium was then submerged in 5 mL of anhydrous toluene in a pre-silanized scintillation vial (presilanization performed by filling the vials with toluene and adding several drops of trichloro-hexyl silane and letting sit overnight before washing with toluene). To this was added 5 μL MEG-Cl. The iridium was then mixed at low speed using a rotoplate for 90 minutes. Then it was rinsed with toluene, and then sonicated in toluene for 5 minutes to remove any excess MEG-Cl.

The iridium was then submerged in 3 mL DCM containing molecular sieves to ensure an anhydrous solution. Added to this was 10 μL 18-Crown-6 Ether. The iridium in solution was rotated overnight on a rotoplate. Then it was copiously rinsed with deionized water and dried under a stream of air.

C. X-Ray Photoelectron Spectroscopy (XPS)

Angle-resolved XPS analysis was performed with a Theta Probe Angle-Resolved X-ray Photoelectron Spectrometer System (Thermo Fisher Scientific Inc., Waltham, MA, USA) located at Surface Interface Ontario (University of Toronto, Toronto, ON, Canada) for iridium plates set aside after cleaning, and each step of chemical surface modification. The samples were analyzed with monochromated Al Kα X-rays (elliptical spots of 400 μm along the long axis) with take-off angles of 90° relative to the surface. Peak fitting and data analysis were performed using the *Avantage* software provided with the instrument.

III. Measurement Setup

The measurements were performed using three different setups: one for preliminary measurements, one while working with fluidic chamber and another one for measurements in artificial cerebrospinal fluid (aCSF).

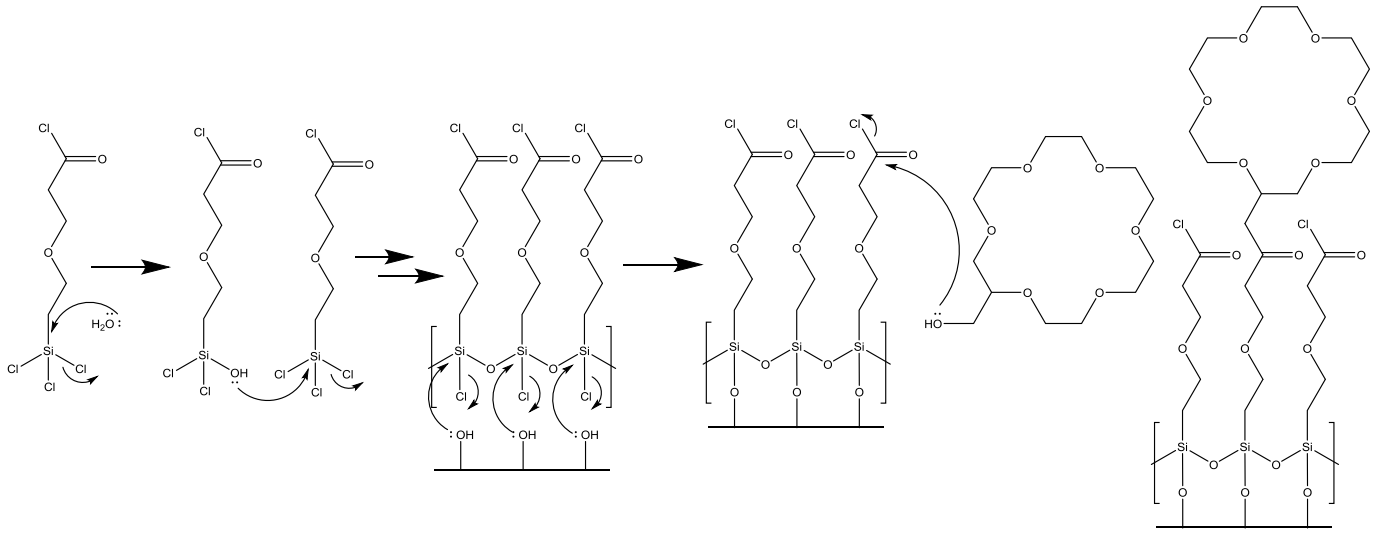

Fig. 1. Modification of hydroxylated surface with an anti-fouling linker (MEG-Cl), and extension with a potassium sensitive probe (crown ether).

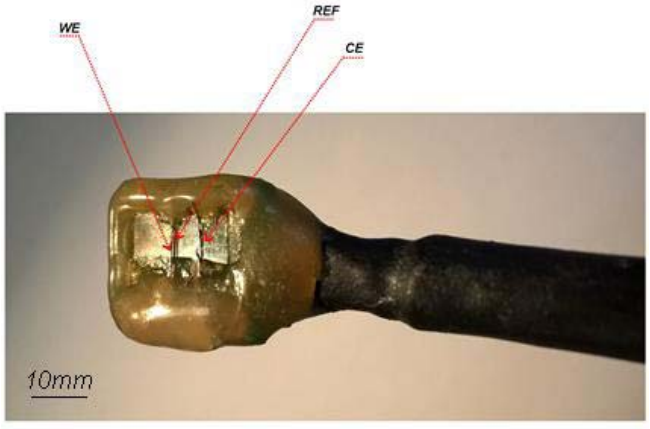

Fig. 2. Sensor used during preliminary measurements: WE – working electrode (coated iridium), REF – pseudo-reference electrode (platinum), CE – counter electrode (platinum).

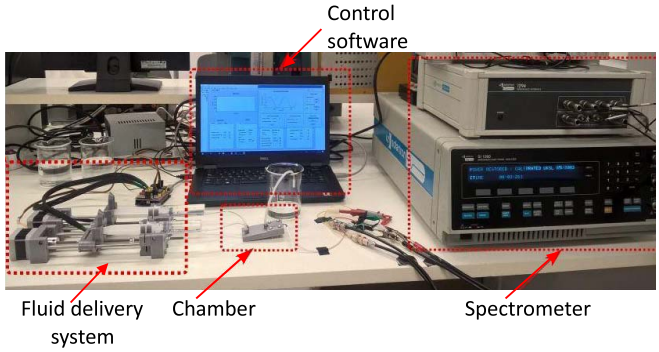

Fig. 3. Measurement setup used during experiments with fluidic chamber.

A. Preliminary Measurement Setup

During preliminary experiments CH Instruments 760E electrochemical Workstation was used to perform measurements. The rest of the equipment included a magnetic stirrer, 11 × 100mL beakers and a laboratory stand.

The sensor consisted of 3 electrodes placed on the polystyrene plate, Fig.2. Three pieces of 0.125mm platinum wire twisted together were used as a counter electrode (CE). A piece of 0.125mm platinum wire served as a pseudo reference electrode (RE). 0.178mm iridium wire coated with K+ sensitive layer served as a working electrode (WE). To make the sensor, a 4-wire (2 twisted pairs) double shielded (with drain wire) cable was used. One twisted pair was used to connect to WE and the RE, one wire from the second pair was used to connect to the CE. Remaining wire was tied to the shield at the device end. The electrodes were glued to the corresponding wires with silver conductive epoxy glue. RE was positioned close to the WE (∼0.5mm) and CE in some distance from those two (∼5mm). The sensor was covered with thick layer of epoxy glue, except the small opening where electrodes were exposed.

B. Fluidic Chamber Measurements Setup

The fluidic system for testing potassium sensors was built to provide the possibility to characterize sensors in controlled, dynamic conditions, Fig.3. This system was used to obtain constant flow of the base fluid in which the concentration of the specified ion changes according to a predefined profile (i.e. sinusoidal, linear, stepwise). The targeted concentrations are obtained by mixing two fluids with different concentration of ions inside the fluidic chamber. The flow of each fluid was digitally controlled with syringe pumps to follow required profile while keeping the total flow rate through the chamber constant at selected level.

The system consisted of four major parts (Fig.3): (a) fluid delivery system, (b) mixing chamber, (c) impedance analyzer and (d) control software. For impedance measurements the Solartron 1260 Impedance Analyzer was used. Fluid delivery system consisted of 2 syringe pumps (custom design based on the open syringe project [21]), and custom-made driver (built around an inexpensive Arduino®platform with CNC shield and Trinamic®TMC2203 motor drivers).

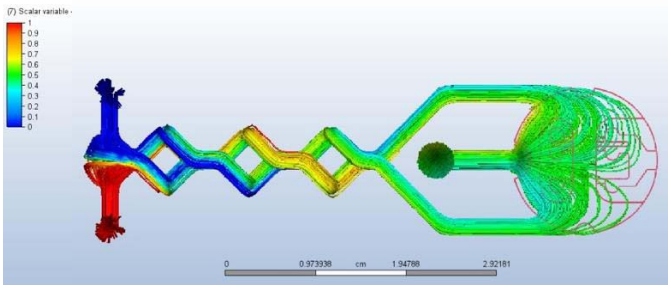

Fig. 4. Flow simulation (Autodesk® CFD).

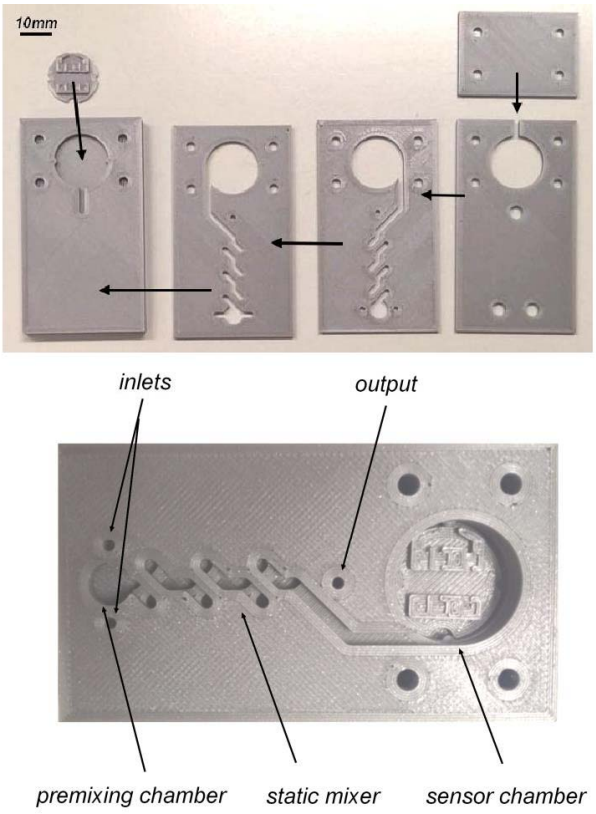

Fig. 5. Fluidic chamber - 3D printed modules (left) and structure of the chamber (right).

Software to control the fluidic system and embedded program for the driver were written using widely available software platforms (AtmelStudio® and VisualStudio®). The impedance analyzer was controlled via custom software written in LabView® environment. All data processing and analysis was performed with Matlab®.

A few different designs were evaluated to minimize material required to manufacture the chamber and to provide appropriate fluid mixing. Prior to manufacturing, *in-silico* studies were performed to ensure the fluids will be mixed in the chamber appropriately (Fig. 4).

The chamber was designed in modular way to enable the use of inexpensive technologies like 3D printing or laser cutting (Fig.5, top). Each module after printing was covered with thin layer of PVB varnish to make the structure waterproof. Modules of the chamber were glued with silicone. The mixing chamber consisted of two inlets, premixing chamber, static mixer, sensor chamber and the output (Fig.5, bottom).

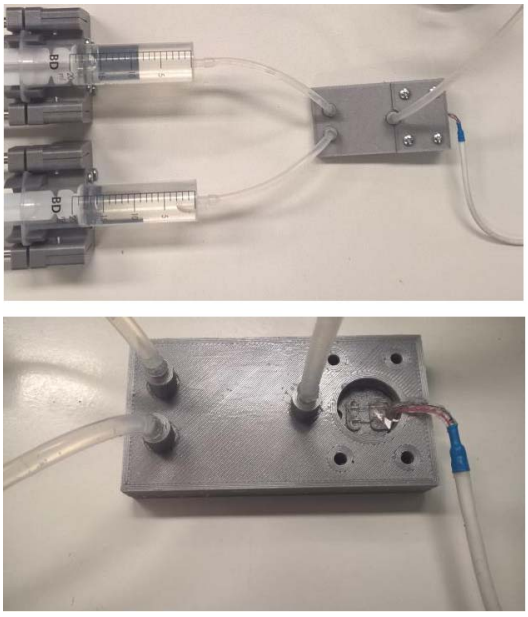

Fig. 6. Chamber connected to syringe pumps with cover (top), and without cover, to show the sensor placement (bottom).

To deliver fluids to the chamber a silicone hose with 4mm outside and 2mm inside diameter was used. The final chamber design is shown at Fig. 6.

The sensor was built in a similar way as during preliminary experiments. However, this time 3D printed support/jig was used. Using the support provides repeatability in electrodes manufacturing. The shape of the support also immobilizes the sensor inside the chamber. The methodology of the electrode manufacturing assumes fabricating a sensor without soldering to avoid unnecessary heating of the electrode wire which could lead to damage of the potassium sensitive coating.

Four ∼7mm pieces of 0.125mm platinum wire were prepared. Three of them were twisted together and placed in the bottom wire socket of the sensor support to serve as a CE electrode. One piece was placed in the middle socket to become RE electrode. A ∼7mm 0.178mm Ir wire coated with K+ sensitive layer was placed in the top socket to serve as a WE. The distance between WE and RE was ∼1mm and between RE and CE ∼ 4mm. A drop of an epoxy glue was placed at the end of each wire (marked a in Fig.7) and in place selected as (b) in Fig.7 to immobilize wires. Next, cable wires were placed into corresponding slots and junctions of wires and electrodes were protected with silver conductive glue. The cable was immobilized by applying epoxy at point c Fig.7. When silver leaving only electrode wires exposed. Finally, connection wires were bent at the right angle and covered with silicone (Fig. 7, right). When electrode is placed in the chamber, silicone around the connection wires serves as a sealant for electrode cable.

C. Artificial Cerebrospinal Fluid (ACSF) Measurements

Impedance measurements were performed using CH Instruments 760E. A frequency of 1 kHz and an AC amplitude of +/- 10 mV was used to measure impedance. A step change

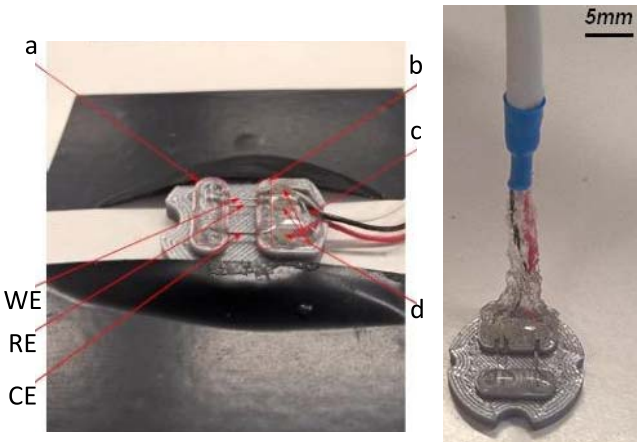

Fig. 7. Sensor during manufacturing (left) – a,b places where epoxy was initially applied, c – place where connecting wires were glued, d – place where silver based conductive glue is applied, WE – working electrode, RE – reference electrode, CE – counter electrode. Sensor with silicone applied to the connecting wires (right).

in concentration of potassium ions and sodium ions was introduced by adding potassium chloride and sodium chloride solutions to ACSF in a controlled manner.

IV. Methods

A. Preliminary Measurements

Impedance measurements were performed using standard 3-electrode configuration at 5kHz, 10mV amplitude, 1S/s. The frequency was chosen based on the impedance spectrum measurements - in the region of phase characteristic transition.

Five 100mL beakers were filled with solutions containing100mM of NaCl and 8mM, 4mM, 2mM, 1mM and 0mM KCl respectively (set 1). Solutions were prepared by serial dilution. Another set of five beakers was filled with solutions containing 108mM, 104mM, 102mM, 101mM and 100mM NaCl respectively (set 2). First, the sensor was placed into the beaker containing DI water for a few minutes. Next, it was placed in the beaker containing 100mM of NaCl and 1mM of KCl for around 60 minutes and during this time the open circuit potential (OCP) was measured. Then, successively beakers were placed on magnetic stirrer in the following order: from one containing lowest concentration of KCl, to one containing highest concentration of KCl and then from highest to lowest (set 1). Every time sensor was immersed in the solution and the recording was taken for around 30s. This sequence was repeated twice. Then the same procedure was repeated for solutions containing only NaCl (set 2).

B. Measurements With the Fluidic Chamber

As in the case of the preliminary experiments impedance measurements were performed using a standard 3-electrode configuration. Parameters used were as follows: frequency 1 kHz, amplitude 10mV, sampling frequency 1S/s. Again, the frequency was chosen based on the impedance spectrum measurements – in the region of phase characteristic transition, this time for a new sensor prepared.

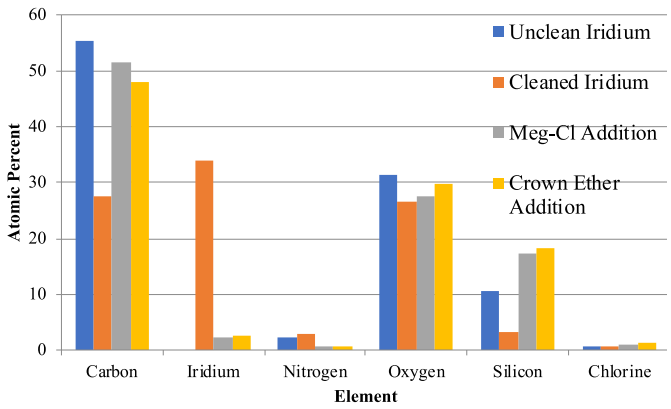

Fig. 8. Elemental composition of iridium surfaces at each stage of modification as measured using XPS.

TABLE I
XPS Percentages From High Resolution Scans for Elemental Composition of Iridium Surfaces at Different Stages of Modification

	Unclean Iridium	*Clean Iridium*	*MEG-Cl Addition*	*Crown Ether Addition*
Carbon	55.38	27.64	51.62	47.99
Iridium	0	33.82	2.3	2.55
Nitrogen	2.17	2.95	0.75	0.63
Oxygen	31.25	26.72	27.39	29.91
Silicon	10.63	3.13	17.22	18.27
Chlorine	0.54	0.64	0.92	1.25

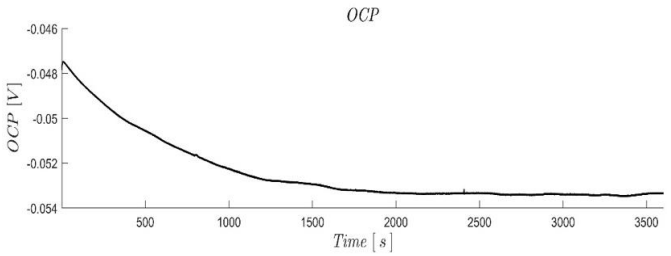

Fig. 9. OCP measured over 60 min. in the solution containing 100mM NaCl and 1mM KCl.

Syringe pumps were used to apply two different patterns of changes in ionic concentration: sinusoidal and pulse. Two solutions were prepared: A, containing 100mM NaCl and B, containing 80mM NaCl and 20mM KCl. The speed of both pumps was controlled differentially. When one pump was speeding up, the second one was slowing down at the same rate, so the total flow through the chamber was held constant at 4ml/min.

In the case of the pulse pattern, for the first 75s only solution A was flowing, then the flow was changed to solution B for 100s and then changed back to solution A for ∼130s. In the case of the sinusoidal pattern, for the first 75s the speed of both pumps was equal, then for next 100s, in a sinusoidal way, the pump containing solution A was slowing down to minimum, speeding up to maximum and then returning to its initial value.

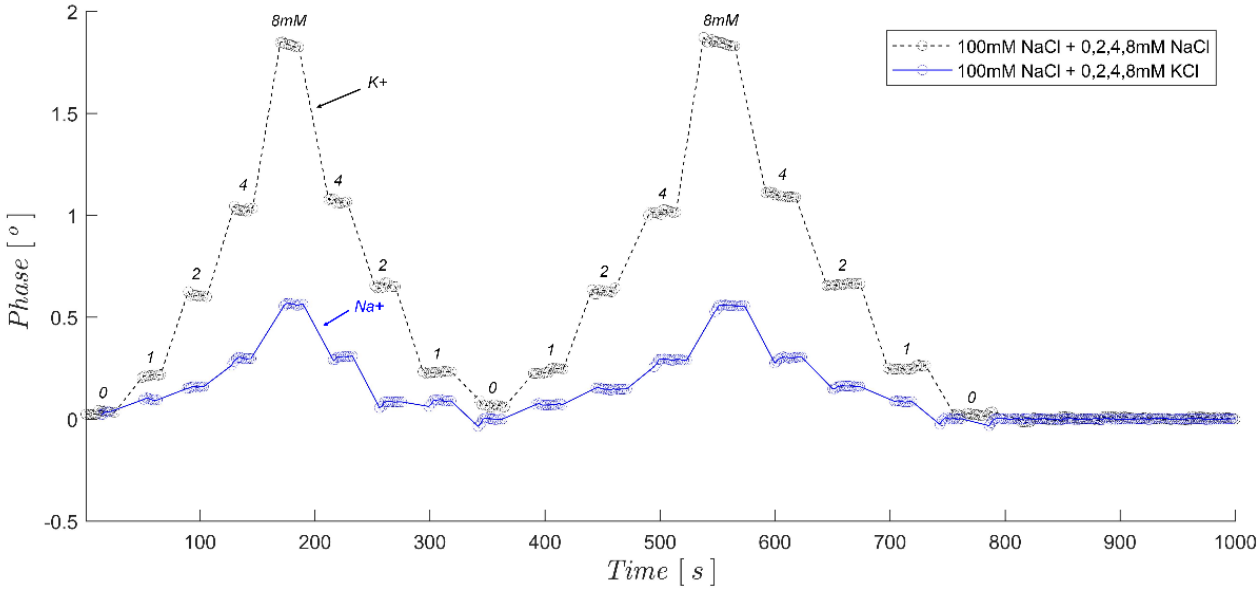

Fig. 10. The sensor response to various potassium and sodium concentrations. Solutions: five beakers with 100mM NaCl and 0, 1, 2, 4 or 8 mM of KCl and for same concentrations of NaCl.

The pump containing solution B was working in opposite way. For last ∼130s the speed of both pumps was equal again. For comparison, the measurements were repeated with both syringe pumps filled with the same solutions containing 100mM NaCl. This was made to ensure that results are not influenced by measurement setup itself (i.e. flow fluctuations).

C. Artificial Cerebrospinal Fluid Measurements

ACSF was made as the following: 124 mM NaCl, 5 mM KCl, 26 mM $NaHCO_3$, 1.25 mM NaH_2PO_4,10 mM D-glucose, 1.3 mM $MgCl_2$, and 1.5 mM $CaCl_2$ in deionized water. The detailed protocol was extracted from [22], [23]. This solution was used as the base fluid to which KCl or NaCl was added in a controlled manner to change the ionic concentration. The sensor was submerged in ACSF for 1 minute for OCP to stabilize, then measurement was made for 5 minutes to measure impedance/phase response of the sensor to the solution. The solutions were subjected to step response changes in concentration of potassium and sodium ions while the phase response was monitored.

V. Results and Discussion

A. Modification of Iridium Wire

XPS analysis was used to verify the surface composition of iridium plates, and thus also the modified iridium wire, at each stage of surface modification. The XPS atomic percentages were calculated from high resolution scans. Detailed values are provided in Table I. The Iridium samples show clear changes to their atomic compositions at each stage of the modification (Fig. 8). Iridium from the package without cleaning was predominantly found to have carbon, oxygen, and silicon on the surface with virtually no iridium signal present. This suggests a large amount of surface contamination as well as possible oxidation of the surface. The iridium signal drastically increased following cleaning, suggesting successful removal of contaminants from the surface.

Following silanization there is a notable increase in carbon and silicon signals, a decrease in iridium signal, as well as a slight increase in chlorine signal. This suggests the successful addition of MEG-Cl to the surface. Finally, addition of the crown ether resulted in a slight decrease in carbon signal, and increase in oxygen signal. This suggests the successful addition of crown ether to the surface, as the ratio of oxygen to carbon is slightly greater in the crown ether, than in the linker.

B. Sensor Use in Buffer Solutions

The OCP measurement results (Fig. 9) indicates that sensor requires more than 30min to stabilize. Over a period of 30 min, the drift in OCP is 3 mV. That suggests the drift in the following measurements, albeit very small, should be expected.

The changes in phase observed during measurements for both sets of solutions (as described in section 4.1) are presented in Fig. 10. The bias value of phase was removed from both measurements to easily compare changes observed. Existing drift in phase was calculated by linear regression of the last minute measurement and subtracted from the data. Data is also inverted for visualisation purposes. The experiment was repeated in both ascending and descending changes of potassium and sodium concentrations to demonstrate repeatability and stability of the sensor measurements.

As can be seen from these measurements, the electrode was moved from solutions with low concentrations of K^+ to those with higher concentrations the phase changed accordingly. When the electrode was moved from high to low concentration the phase returned almost perfectly to the previously observed baseline. This process could be repeated multiple times, with the phase corresponding well to the concentration of K^+ in each solution. Solutions containing differing concentrations of

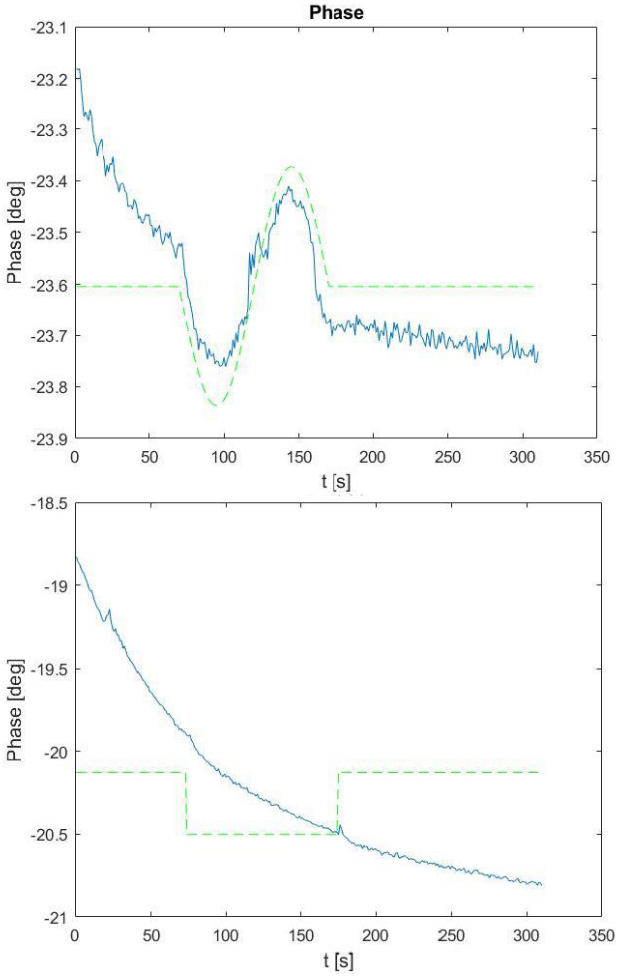

Fig. 11. (Top) Response for sinusoidal change of K^+ concentration. 100mM NaCl solution was mixed with 80mM NaCl + 20mM KCl solution. Potassium concentration profile (green-broken line, reversed for visualization purpose) has the amplitude of 20mM pk-pk and period of 100s. Blue line shows the measured values. (bottom) Control measurement: two identical solutions (100mM NaCl) were used. Green line corresponds to the action of the syringe pumps identical as in case of previous measurements. Blue line shows the measured values.

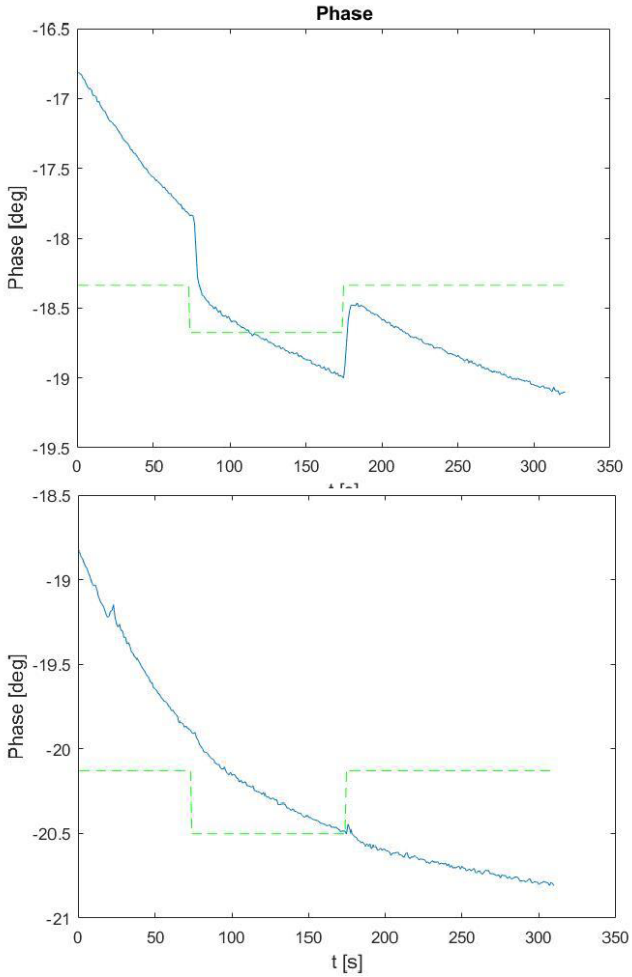

Fig. 12. (Top) Response for step change of K^+ concentration. 100mM NaCl solution was mixed with 80mM NaCl + 20mM KCl solution. Potassium concentration step change (green-broken line, reversed for visualization purpose) has the amplitude of 20mM and duration time of 100s. Blue line shows the measured values. (Bottom) Control measurement: two identical solutions (100mM NaCl) were used. Green line corresponds to the action of the syringe pumps identical as in case of previous measurements. Blue line shows the measured values.

Na^+ also showed phase changes which corresponded to the concentration, however these changes were much smaller than those observed for K^+. This suggests that the measurements are fairly specific to K^+ as well as reproducible.

The chosen range of potassium concentrations corresponds to the relevant physiological range for the *extracellular* K^+ concentrations. For plasma concentrations, the normal range is 3.5 mM – 5 mM, and the highest reported concentration during strenuous exercise was around 8 mM [24]. The concentration of K^+ in the CSF of healthy mammals is about 2.5 mM – 4 mM [25], and measurements made in unstimulated brain and spinal cord confirm the baseline of up to 4 mM, and in epileptic seizures of around 12 mM [26].

C. Sensor Characterized in Fluidic Chamber

To demonstrate that the sensor is able to measure continuously changing concentration of the ions over time, and not just measure drastically different concentrations as in the previous experiment, we have performed experiments using our fluidic chamber. Results of measurements with the fluidic chamber are presented in Fig. 11 and 12.

In Fig. 11 the response for sinusoidal change in K^+ concentration is shown. In Fig. 12 the response for step change is presented. The green line represents when the concentration changes were applied and the pattern used (aligned manually to compensate the lag resulting from chamber volume). It can be observed that phase follows the changes of potassium concentration. The response for control measurements are not visible. That ensures that results obtained are not influenced by measurement setup itself.

The fluidic chamber allows for frequency characterization of chemical sensors. Here (Fig.11) we demonstrate it only for one frequency which corresponds to the period of 100s.

D. Sensor Tested in Artificial Cerebrospinal Fluid

We have also tested the sensor in ACSF in order to determine if it works in biological solutions (Fig. 13). As can be

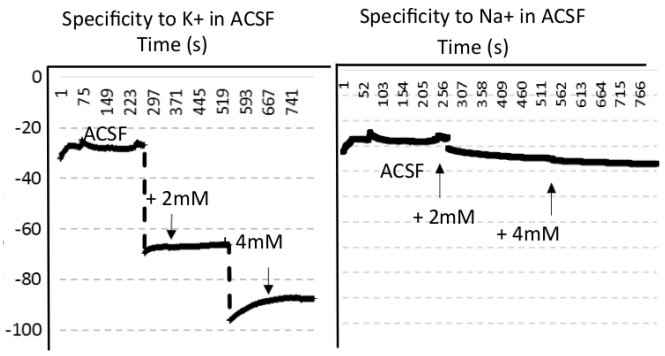

Fig. 13. Shows the comparison of the sensor measurements for increasing concentrations of K^+ (left) and Na^+ (right) in artificial cerebrospinal fluid (aCSF).

seen from the data the sensor showed a much larger response to changes in K^+ concentration in this simulated biological fluid, compared to Na^+. This shows that not only is the sensor able to operate in a more complicated matrix, which would cause far more surface fouling than the previously tested buffer solutions, but that it is still very selective to K^+ in this solution. This gives great promise for the sensor being used successfully *in vivo*.

For the measurement instrumentation and custom-made calibration used in our experiments, the sensor can reliably and reproducibly detect at least 1 mM potassium concentration change, with the lower limit of sensitivity of 0.5 mM.

Our previous acute study [6] involving Ir-based microwire electrode indicates no significant difference in and adverse effect to neural responses pre and post implantation. Significant damage is not expected for brain studies, since the electrode dimension is of a similar size of typical electrodes used for brain neural recordings, such as Utah array [27].

VI. Conclusion

The present work shows that it is possible to coat iridium oxide metal with trichlorosilane surface coatings. In this case, an anti-fouling linker which was extended with a potassium sensitive probe. This modified iridium wire can then be used as the basis for a potassium sensitive impedance sensing electrode, which provides highly sensitive and reproducible results. The validation platform described enabled successful dynamic characterization of the sensor and helped in determining the dynamic response of the sensor to various temporal types (step/sinusoidal) changes in K^+ concentration. The electrode was found to not only operate successfully in buffer solutions, but also in artificial cerebrospinal fluid indicating that it could be adapted for use in living nerve bundles. The next step will be to develop and test an implantable version of this electrode for use in *in vivo* potassium sensing.

References

[1] M. Thompson, "Neurophysiological monitoring of potassium," in *Compendium of* in Vivo *Monitoring in Real-Time Molecular Neuroscience*, vol. 3, G. Wilson and A. Michael, Eds. Singapore: World Scientific, 2020, pp. 293–323.

[2] F. Suga, T. Nakashima, and J. B. Snow, "Sodium and potassium ions in endolymph: *in vivo* measurements with glass microelectrodes," *Arch. Otolaryngol.—Head Neck Surgery*, vol. 91, no. 1, pp. 37–43, Jan. 1970.

[3] U. Heinemann, H. D. Lux, and M. J. Gutnick, "Extracellular free calcium and potassium during paroxysmal activity in the cerebral cortex of the cat," *Express Brain Res.*, vols. 27–27, nos. 3–4, pp. 237–243, Mar. 1977.

[4] H. Bischof *et al.*, "Novel genetically encoded fluorescent probes enable real-time detection of potassium *in vitro* and *in vivo*," *Nature Commun.*, vol. 8, no. 1, Dec. 2017, article no. 1422, doi: 10.1038/s41467-017-01615-z.

[5] S. Dufour, P. Dufour, O. Chever, R. Vallée, and F. Amzica, "*in vivo* simultaneous intra- and extracellular potassium recordings using a micro-optrode," *J. Neurosci. Methods*, vol. 194, no. 2, pp. 206–217, Jan. 2011.

[6] S. C. Cork *et al.*, "Extracellular pH monitoring for use in closed-loop vagus nerve stimulation," *J. Neural Eng.*, vol. 15, no. 1, Feb. 2018, Art. no. 016001.

[7] K. B. Mirza, C. T. Golden, K. Nikolic, and C. Toumazou, "Closed-loop implantable therapeutic neuromodulation systems based on neurochemical monitoring," *Frontiers Neurosci.*, vol. 13, p. 808, Aug. 2019.

[8] T. Xiao, F. Wu, J. Hao, M. Zhang, P. Yu, and L. Mao, "*in vivo* analysis with electrochemical sensors and biosensors," *Anal. Chem.*, vol. 89, no. 1, pp. 300–313, Jan. 2017.

[9] W. Endres, P. Grafe, H. Bostock, and G. Ten Bruggencate, "Changes in extracellular pH during electrical stimulation of isolated rat vagus nerve," *Neurosci. Lett.*, vol. 64, no. 2, pp. 201–205, Feb. 1986.

[10] R. Machado *et al.*, "Biofouling-resistant impedimetric sensor for array high-resolution extracellular potassium monitoring in the brain," *Biosensors*, vol. 6, no. 4, p. 53, Oct. 2016.

[11] Q. Liu, A. Singh, R. Lalani, and L. Liu, "Ultralow fouling polyacrylamide on gold surfaces via surface-initiated atom transfer radical polymerization," *Biomacromolecules*, vol. 13, no. 4, pp. 1086–1092, Apr. 2012.

[12] S. Sheikh, D. Y. Yang, C. Blaszykowski, and M. Thompson, "Single ether group in a glycol-based ultra-thin layer prevents surface fouling from undiluted serum," *Chem. Commun.*, vol. 48, no. 9, pp. 1305–1307, 2012.

[13] M. B. More, D. Ray, and P. B. Armentrout, "Intrinsic affinities of alkali cations for 15-Crown-5 and 18-Crown-6: Bond dissociation energies of gas-phase M+a'Crown ether complexes," *J. Amer. Chem. Soc.*, vol. 121, no. 2, pp. 417–423, Jan. 1999.

[14] P. Benvenuto, "Adlayer-mediated antibody immobilization to stainless steel for potential application to endothelial progenitor cell capture," *Langmuir*, vol. 31, no. 19, pp. 5423–5431, 2015.

[15] B. De La Franier, A. Jankowski, and M. Thompson, "Functionalizable self-assembled trichlorosilyl-based monolayer for application in biosensor technology," *Appl. Surf. Sci.*, vol. 414, pp. 435–441, Aug. 2017.

[16] K. B. Mirza, N. Kulasekeram, Y. Liu, K. Nikolic, and C. Toumazou, "System on chip for closed loop neuromodulation based on dual mode biosignals," in *Proc. IEEE Int. Symp. Circuits Syst. (ISCAS)*, Sapporo, Japan, May 2019, pp. 1–5.

[17] B. Bozorgzadeh, D. R. Schuweiler, M. J. Bobak, P. A. Garris, and P. Mohseni, "Neurochemostat: A neural interface SoC with integrated chemometrics for closed-loop regulation of brain dopamine," *IEEE Trans. Biomed. Circuits Syst.*, vol. 10, no. 3, pp. 654–667, Jun. 2016.

[18] K. B. Mirza *et al.*, "Influence of cholecystokinin-8 on compound nerve action potentials from ventral gastric vagus in rats," *Int. J. Neural Syst.*, vol. 28, no. 9, 2018, Art. no. 1850006.

[19] C. Zuliani, F. S. Ng, A. Alenda, A. Eftekhar, N. S. Peters, and C. Toumazou, "An array of individually addressable micro-needles for mapping pH distributions," *Analyst*, vol. 141, no. 15, pp. 4659–4666, 2016.

[20] N. Moser *et al.*, "CMOS potentiometric FET array platform using sensor learning for multi-ion imaging," *Anal. Chem.*, vol. 92, pp. 5276–5285, 2020, doi: 10.1021/acs.analchem.9b05836.

[21] B. Wijnen, E. J. Hunt, G. C. Anzalone, and J. M. Pearce, "Open-source syringe pump library," *PLoS ONE*, vol. 9, no. 9, Sep. 2014, Art. no. e107216.

[22] J. Hrabe and S. Hrabetova, "Time-resolved integrative optical imaging of diffusion during spreading depression," *Biophys. J.*, vol. 117, no. 10, pp. 1783–1794, Nov. 2019.

[23] S. C. Cork, J. E. Richards, M. K. Holt, F. M. Gribble, F. Reimann, and S. Trapp, "Distribution and characterisation of glucagon-like peptide-1 receptor expressing cells in the mouse brain," *Mol. Metabolism*, vol. 4, no. 10, pp. 718–731, Oct. 2015.

[24] C.-J. Cheng, E. Kuo, and C.-L. Huang, "Extracellular potassium homeostasis: Insights from hypokalemic periodic paralysis," *Seminars Nephrol.*, vol. 33, no. 3, pp. 237–247, May 2013.

[25] G. G. Somjen, "Extracellular potassium in the mammalian central nervous system," *Annu. Rev. Physiol.*, vol. 41, no. 1, pp. 159–177, Oct. 1979.
[26] J. V. Raimondo, R. J. Burman, A. A. Katz, and C. J. Akerman, "Ion dynamics during seizures," *Front. Cell. Neurosci.*, vol. 9, p. 419, Dec. 2015, doi: 10.3389/fncel.2015.00419.
[27] H. A. C. Wark *et al.*, "A new high-density (25 electrodes/mm^2) penetrating microelectrode array for recording and stimulating sub-millimeter neuroanatomical structures," *J. Neural Eng.*, vol. 10, no. 4, Aug. 2013, Art. no. 045003.

Krzysztof Wildner received the M.Sc.Eng. degree in automatic control and robotics and the Ph.D. degree in biocybernetics and biomedical engineering from the Faculty of Mechatronics, Warsaw University of Technology. From 2017 to 2018, he was a Research Associate with the Centre for Bio-Inspired Technology, Imperial College London, and taking part as a Postdoctoral Researcher in the ERC project. He is an Assistant Professor with the Institute of Metrology and Biomedical Engineering, Warsaw University of Technology. His research interests include neuroprosthetics, biorobotics, and sensing technology for linking the body with technical devices. For his Ph.D. thesis, he received the Siemens Award.

Khalid Baig Mirza (Member, IEEE) received the Ph.D. degree from the Centre for Bio-Inspired Technology (CBIT), Department of EE, Imperial College London in 2018, under the supervision of Prof. Christofer Toumazou, focusing on developing system-on-chip (SoC) for closed-loop vagus nerve stimulation (VNS) for treating obesity. He is a Postdoctoral Research Associate with CBIT, Department of Electrical and Electronic Engineering (EE), Imperial College London. His current research interests include developing efficient, small-size, implantable, closed-loop neuromodulators, and neurochemical sensors for electroceutical applications. Prior to working in academia, he worked in industry as an Electronics Engineer in the Product Design Team, to implement a novel authentication technology called Laser Surface Authentication (LSA). His work at Imperial has been funded through the European Research Council (ERC) and the Engineering and Physical Sciences Research Council (EPSRC) grants.

Brian de La Franier received the bachelor's degree from the University of Toronto in 2012, a specialist in biological chemistry, focusing primarily on protein and artificial blood synthesis, and the Ph.D. degree in 2017. He is a Postdoctoral Research Associate with the University of Toronto. He began his Ph.D. in 2012 studying the development of new ovarian cancer detection techniques in serum under the supervision of Prof. Michael Thompson. After a short time in other pursuits returned to Prof. Thompson's lab to work as a Postdoctoral Fellow studying the reduction in bacterial adhesion to surfaces, which he continues to this day. He works primarily as a surface chemist, modifying surfaces for use in biosensors and medical applications. He performs the necessary chemical synthesis and analysis, protein synthesis, and surface analysis.

Simon Cork received the bachelor's and Ph.D. degrees in biomedical science and neuroscience from Durham University. He held a Research Fellowship at the Department of Medicine, Imperial College London, preceded by a research associate position at the University College London, where his research focused on the neural regulation of appetite. He is a Neurophysiologist and a Medical Educator. He is currently a Teaching Fellow in Medical Education with the King's College London Medical School and an Honorary Lecturer with the Department of Investigative Medicine, Imperial College London. His research has focused on the role of the vagus nerve in gut–brain communications and the development of neural stimulating devices for the treatment of obesity.

Christofer Toumazou (Fellow, IEEE) is currently the Founding Director and a Chief Scientist with the Institute of Biomedical Engineering, Imperial College London, London, U.K., where he is also the Research Director of the Centre for Bio-Inspired Technology and the Winston Wong Chair of Biomedical Circuits with the Department of Electrical and Electronic Engineering. He is the Founder of three technology-based companies with applications spanning ultralow-power mobile technology (Toumaz Technology Ltd., U.K.), DNA sequencing (DNA Electronics Ltd., U.K.), and geneOnyx Ltd., a company applying the DNAe technology to retail cosmetics. He has authored more than 700 research articles and holds more than 40 patents in the field of semiconductors and healthcare many of which are currently fully granted PCT. He is distinguished for his groundbreaking innovations in silicon technology and integrated circuit design. His career began with the invention and development of the entirely novel concept of current-mode analog circuitry for ultralow-power electronic devices. For this, he became one of the youngest ever professors at Imperial College London. However, it has been his success in applying silicon chip technology to biomedical and life-science applications, most recently to DNA analysis, that is leading to new innovations in the field of genetics, molecular biology, and personalized medicine. In 2008, he was appointed as a Fellow of the Royal Academy of Engineering and the Royal Society. In 2013, he was a Fellow of the Academy of Medical Sciences and was conferred the title of Regius Professor in the Queens 2012 Diamond Jubilee. He has received many awards, including the Royal Society Clifford Patterson Prize Lecture, entitled The Bionic Man, for which he received the Royal Society Clifford Patterson Bronze Medal in 2003. He was a recipient of the 2005 IEEE CAS Education Award for pioneering contributions in circuits and systems for biomedical applications, the Royal Academy of Engineering Silver Medal in 2007 for pioneering contributions to the British industry, the World Technology Award from *Time* (Magazine) for the Health and Medicine category in 2009, the 2011 J. J. Thompson Medal of the Institution of Engineering and Technology, and the European Inventor Award from the European Patent.

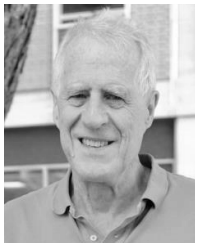

Michael Thompson (Member, IEEE) received the bachelor's degree from the University of Wales, U.K., and the Ph.D. degree in analytical chemistry from McMaster University. Following a period as a Science Research Council PDF at Swansea University, he was appointed as a Lecturer of Instrumental Analysis at Loughborough University. He then moved to the University of Toronto, where he is a Professor of Bioanalytical Chemistry. He is a Professor of Bioanalytical Chemistry with the University of Toronto. He has held a number of distinguished research posts, including the Leverhulme Fellowship at Durham University and the Science Foundation Ireland E. T. S. Walton Research Fellowship at the Tyndall National Institute, Cork City. He is recognized internationally for his pioneering work over many years in the area of research into new biosensor technologies and the surface chemistry of biochemical and biological entities. He has made major contributions to the label-free detection of biological macromolecule interactions and surface behavior of cells using ultrahigh-frequency acoustic wave physics. He has also pioneered the development of antifouling surface modification, in particular anti-thrombogenic and antimicrobial adhesion materials. He was made a Fellow of the Royal Society of Canada in 1999. He has been awarded many prestigious international prizes for his research, including the Robert Boyle Gold Medal of the Royal Society of Chemistry, the E. W. R. Steacie Award of the Chemical Society of Canada, the Theophilus Redwood Award of the Royal Society of Chemistry, and the Fisher Scientific Award in Analytical Chemistry of the Chemical Society of Canada. He has served on the Editorial Boards for a number of major international journals, including *Analytical Chemistry*, *Analyst*, *Talanta*, *Analytica Chimica Acta*, and *Biosensors and Bioelectronics*. He is the Editor-in-Chief of the monograph series Detection Science for the Royal Society of Chemistry, U.K.

Konstantin Nikolic (Member, IEEE) received the Dipl.Eng. and master's degrees in applied physics from the University of Belgrade, Serbia, and the Ph.D. degree in physics from Imperial College London, U.K. He was an Assistant Professor and then an Associate Professor with the Faculty of Electrical Engineering, University of Belgrade. He was an Associate Professor–Research (Senior Research Fellow) and a Principal Investigator with the Institute of Biomedical Engineering and Department of Electrical and Electronic Engineering, Imperial College London from 2006 to 2020. He is a Professor of Computing Science: Artificial Intelligence, Machine Learning and Data Management with the School of Computing and Engineering, University of West London, London, U.K. He leads the Learning and Intelligence in Biological Systems and Machines Group, which develops methods and computational tools for understanding, modeling, and simulating various biological and physiological processes and their applications in bio-inspired electronic systems and diagnostics. He also leads the research programme which is developing a closed-loop system for bimodal neural recording and neuro-stimulation. He has more than 100 scientific publications and is a coauthor of several widely used university textbooks. He is a member of the IEEE CAS Technical Committee and the Royal Society Neural Interfaces Steering Group. He is an Associate Editor of *Frontiers in Neuroscience*, specialty Neuromorphic Engineering and the IEEE TRANSACTIONS ON BIOMEDICAL CIRCUITS AND SYSTEMS (TBioCAS).